Enhancing and controlling single-atom high-harmonic generation spectra: a time-dependent density-functional scheme

Alberto Castro[1,2,*]**, Angel Rubio**[3]**, and E. K. U. Gross**[4]

[1]*ARAID Foundation, Edificio CEEI, María de Luna s/n, 50018 Zaragoza Spain*
[2]*Institute for Biocomputation and Physics of Complex Systems (BIFI), and Zaragoza Center for Advanced Modelling (ZCAM), University of Zaragoza, 50018 Zaragoza, Spain*
[3]*Nano-Bio Spectroscopy Group and ETSF Scientific Development Centre, Departamento de Física de Materiales, Centro de Física de Materiales CSIC-UPV/EHU-MPC and DIPC, Universidad del País Vasco UPV/EHU, E-20018 San Sebastián, Spain*
[4]*Max-Planck Institut für Mikrostrukturphysik, Weinberg 2, D-06120 Halle, Germany*
[*]acastro@bifi.es

Abstract: High harmonic generation (HHG) provides a flexible framework for the development of coherent light sources in the extreme-ultraviolet and soft x-ray regimes. However it suffers from low conversion efficiencies as the control of the HHG spectral and temporal characteristics requires manipulating electron trajectories on attosecond time scale. The phase matching mechanism has been employed to selectively enhance specific quantum paths leading to HHG. A few important fundamental questions remain open, among those how much of the enhancement can be achieved by the single-emitter and what is the role of correlations (or the electronic structure) in the selectivity and control of HHG generation. Here we address those questions by examining computationally the possibility of optimizing the HHG spectrum of isolated Hydrogen and Helium atoms by shaping the slowly varying envelope of a 800 nm, 200-cycles long laser pulse. The spectra are computed with a fully quantum mechanical description, by explicitly computing the time-dependent dipole moment of the systems using a first-principles time-dependent density-functional approach (exact for the case of H). The sought optimization corresponds to the selective enhancement of single harmonics, which we find to be significant. This selectivity is entirely due to the single atom response, and not due to any propagation or phase-matching effect. In fact, this single-emitter enhancement adds to the phase-matching techniques to achieving even larger HHG enhancement factors. Moreover, we see that the electronic correlation plays a role in the determining the degree of optimization that can be obtained.

OCIS codes: (000.0000) General.

References and links

1. P. A. Franken, A. E. Hill, C. W. Peters, and G. Weinreich, "Generation of optical harmonics," Physical Review Letters **7**, 118–119 (1961).

2. A. McPherson, G. Gibson, H. Jara, U. Johann, T. S. Luk, I. A. McIntyre, K. Boyer, and C. K. Rhodes, "Studies of multiphoton production of vacuum-ultraviolet radiation in the rare gases," Journal of the Optical Society of America B **4**, 595–601 (1987).

3. M. Ferray, A. L. Huillier, X. F. Li, L. A. Lompré, G. Mainfray, and C. Manus, "Multiple-harmonic conversion of 1064 nm radiation in rare gases," Journal of Physics B: Atomic, Molecular and Optical Physics **21**, L31–L35 (1988).

4. O. Smirnova and M. Ivanov, "Multielectron High Harmonic Generation: simple man on complex plane," arXiv preprint arXiv:1304.2413v1 (2013).

5. K. L. Ishikawa, "High-Harmonic Generation," in "Advances in Solid State Lasers Development and Applications," , M. Grishin, ed. (Intech, 2010), February, chap. 19, pp. 439–464.

6. M. Hentschel, R. Kienberger, C. Spielmann, G. A. Reider, N. Milosevic, T. Brabec, P. Corkum, U. Heinzmann, M. Drescher, and F. Krausz, "Attosecond metrology," Nature **414**, 509–513 (2001).

7. A. Wirth, M. T. Hassan, I. Grgura, J. Gagnon, A. Moulet, T. T. Luu, S. Pabst, R. Santra, Z. A. Alahmed, A. M. Azzeer, V. S. Yakovlev, V. Pervak, F. Krausz, and E. Goulielmakis, "Synthesized light transients," Science **334**, 195–200 (2011).

8. T. Brabec and F. Krausz, "Intense few-cycle laser fields: Frontiers of nonlinear optics," Reviews of Modern Physics **72**, 545–591 (2000).

9. M. Drescher, M. Hentschel, R. Kienberger, M. Uiberacker, V. Yakovlev, A. Scrinzi, T. Westerwalbesloh, U. Kleineberg, U. Heinzmann, and F. Krausz, "Time-resolved atomic inner-shell spectroscopy," Nature **419**, 803–807 (2002).

10. D. Lee, J.-H. Kim, K.-H. Hong, and C. Nam, "Coherent Control of High-Order Harmonics with Chirped Femtosecond Laser Pulses," Physical Review Letters **87**, 243902 (2001).

11. Z. Chang, A. Rundquist, H. Wang, M. M. Murnane, and H. C. Kapteyn, "Generation of coherent soft x rays at 2.7 nm using high harmonics," Phys. Rev. Lett. **79**, 2967–2970 (1997).

12. H. T. Kim, D. G. Lee, K.-H. Hong, J.-H. Kim, I. W. Choi, and C. H. Nam, "Continuously tunable high-order harmonics from atoms in an intense femtosecond laser field," Phys. Rev. A **67**, 051801 (2003).

13. A. M. Weiner, "Femtosecond pulse shaping using spatial light modulators," Review of Scientific Instruments **71**, 1929 (2000).

14. C. Brif, R. Chakrabarti, and H. Rabitz, "Control of quantum phenomena: past, present and future," New Journal of Physics **12**, 075008 (2010).

15. C. Winterfeldt, C. Spielmann, and G. Gerber, "Colloquium: Optimal control of high-harmonic generation," Reviews of Modern Physics **80**, 117–140 (2008).

16. R. Bartels, S. Backus, E. Zeek, L. Misoguti, G. Vdovin, I. P. Christov, M. M. Murnane, and H. C. Kapteyn, "Shaped-pulse optimization of coherent emission of high-harmonic soft X-rays," Nature **406**, 164 (2000).

17. R. Bartels, S. Backus, I. Christov, H. Kapteyn, and M. Murnane, "Attosecond time-scale feedback control of coherent x-ray generation," Chemical Physics **267**, 277 – 289 (2001).

18. T. Pfeifer, D. Walter, C. Winterfeldt, C. Spielmann, and G. Gerber, "Controlling the spectral shape of coherent soft X-rays," Applied Physics B **80**, 277–280 (2005).

19. D. H. Reitze, S. Kazamias, F. Weihe, G. Mullot, D. Douillet, F. Augé, O. Albert, V. Ramanathan, J. P. Chambaret, D. Hulin, and P. Balcou, "Enhancement of high-order harmonic generation at tuned wavelengths through adaptive control." Optics letters **29**, 86–8 (2004).

20. P. Villoresi, S. Bonora, M. Pascolini, L. Poletto, G. Tondello, C. Vozzi, M. Nisoli, G. Sansone, S. Stagira, and S. D. Silvestri, "Optimization of high-order harmonic generation by adaptive control of a sub-10-fs pulse wave front," Opt. Lett. **29**, 207–209 (2004).

21. D. Walter, "Adaptive control of ultrashort laser pulses for high-harmonic generation," Ph.D. thesis, University of Wüürzburg (2006).

22. A. Paul, R. A. Bartels, R. Tobey, H. Green, S. Weiman, I. P. Christov, M. M. Murnane1, H. C. Kapteyn, and S. Backus, "Quasi-phase-matched generation of coherent extreme-ultraviolet light," Nature **421**, 51–54 (2003).

23. J. Werschnik and E. K. U. Gross, "Quantum optimal control theory," Journal of Physics B: Atomic, Molecular and Optical Physics **40**, R175 – R211 (2007).

24. I. Schaefer and R. Kosloff, "Optimal-control theory of harmonic generation," Physical Review A **86**, 063417 (2012).

25. I. Schaefer, "Quantum optimal control theory of harmonic generation," Master's thesis, Fritz Haber Center, Institute of Chemistry, The Hebrew University of Jerusalem (2012).

26. J. L. Krause, K. J. Schafer, and K. C. Kulander, "High-Order Harmonic Generation from Atoms and Ions in the High Intensity Regime," Physical Review Letters **68**, 3535 (1992).

27. K. J. Schafer, B. Yang, L. F. DiMauro, and K. C. Kulander, "Above threshold ionization beyond the high harmonic cutoff," Phys. Rev. Lett. **70**, 1599–1602 (1993).

28. P. B. Corkum, "Plasma perspective on strong field multiphoton ionization," Phys. Rev. Lett. **71**, 1994–1997 (1993).

29. M. Lewenstein, P. Balcou, M. Y. Ivanov, A. L'Huillier, and P. B. Corkum, "Theory of high-harmonic generation by low-frequency laser fields," Physical Review A **49**, 2117 (1994).

30. K. Kulander, K. Schafer, and J. Krause, "Theoretical model for intense field high-order harmonic generation in rare gases," Laser Phys **3**, 359–364 (1993).
31. X.-M. Tong and S.-I. Chu, "Theoretical study of multiple high-order harmonic generation by intense ultrashort pulsed laser fields: A new generalized pseudospectral time-dependent method," Chemical Physics **217**, 119 – 130 (1997). ¡ce:title¿Dynamics of Driven Quantum Systems¡/ce:title¿.
32. a. Bandrauk, S. Chelkowski, D. Diestler, J. Manz, and K.-J. Yuan, "Quantum simulation of high-order harmonic spectra of the hydrogen atom," Physical Review A **79**, 023403 (2009).
33. A. Gordon, F. X. Kärtner, N. Rohringer, and R. Santra, "Role of many-electron dynamics in high harmonic generation," Phys. Rev. Lett. **96**, 223902 (2006).
34. S. Pabst and R. Santra, "Strong-field many-body physics and the giant enhancement in the high-harmonic spectrum of xenon," Phys. Rev. Lett. **111**, 233005 (2013).
35. E. Runge and E. Gross, "Density-functional theory for time-dependent systems," Physical Review Letters **52**, 997–1000 (1984).
36. M. A. L. Marques, N. T. Maitra, F. M. S. Nogueira, E. K. U. Gross, and A. Rubio, eds., *Fundamentals of Time-Dependent Density Functional Theory*, vol. 837 of *Lecture Notes in Physics* (Springer, Berlin Heidelberg, 2012).
37. C. A. Ullrich, S. Erhard, and E. K. U. Gross, "Time-dependent density-functional approach to atoms in strong laser pulses," in "Super Intense Laser Atom Physics IV," , H. G. Muller and M. V. Fedorov, eds. (Kluwer, 1996), NATO ASI Series 3/13, pp. 267–284.
38. M. A. L. Marques, A. Castro, G. F. Bertsch, and A. Rubio, "octopus: a first-principles tool for excited electron-ion dynamics," Computer Physics Communications **151**, 60–78 (2003).
39. A. Castro, H. Appel, M. Oliveira, C. A. Rozzi, X. Andrade, F. Lorenzen, M. A. L. Marques, E. K. U. Gross, and A. Rubio, "octopus: a tool for the application of timedependent density functional theory," Physica Status Solidi (b) **243**, 2465–2488 (2006).
40. B. Sundaram and P. W. Milonni, "High-order harmonic generation: Simplified model and relevance of single-atom theories to experiment," Physical Review A **41**, 6571–6573 (1990).
41. J. I. Fuks, P. Elliott, A. Rubio, and N. T. Maitra, "Dynamics of charge-transfer processes with time-dependent density functional theory," The Journal of Physical Chemistry Letters **4**, 735–739 (2013).
42. A. Castro, J. Werschnik, and E. Gross, "Controlling the Dynamics of Many-Electron Systems from First Principles: A Combination of Optimal Control and Time-Dependent Density-Functional Theory," Physical Review Letters **109**, 153603 (2012).
43. M. J. D. Powell, "Developments of NEWUOA for minimization without derivatives," IMA Journal of Numerical Analysis **28**, 649–664 (2008).
44. K. Krieger, A. Castro, and E. K. U. Gross, "Optimization Schemes for Selective Molecular Cleavage with Tailored Ultrashort Laser Pulses," Chemical Physics **391**, 51 (2011).
45. C.-G. Wahlström, J. Larsson, A. Persson, T. Starczewski, S. Svanberg, P. Salières, P. Balcou, and A. L'Huillier, "High-order harmonic generation in rare gases with an intense short-pulse laser," Phys. Rev. A **48**, 4709–4720 (1993).
46. E. Constant, D. Garzella, P. Breger, E. Mével, C. Dorrer, C. Le Blanc, F. Salin, and P. Agostini, "Optimizing high harmonic generation in absorbing gases: Model and experiment," Phys. Rev. Lett. **82**, 1668–1671 (1999).
47. A. Gordon, F. X. Kärtner, N. Rohringer, and R. Santra, "Role of many-electron dynamics in high harmonic generation," Phys. Rev. Lett. **96**, 223902 (2006).
48. A. Castro, M. Marques, and A. Rubio, "Propagators for the time-dependent KohnSham equations," The Journal of chemical physics **121** (2004).
49. A. Castro, M. Isla, J. Martínez, and J. Alonso, "Scattering of a proton with the Li 4 cluster: Non-adiabatic molecular dynamics description based on time-dependent density-functional theory," Chemical Physics **399**, 130–134 (2012).

1. Introduction

At sufficiently high intensities, matter no longer reacts linearly to light, and may re-emit at integer multiples (*harmonics*) of the frequency of the incoming source [1]. According to perturbation theory, the intensity of the harmonics decreases exponentially with their order. However, the spectrum of atoms and molecules exposed to very intense, typically infrared, laser pulses was found to present unexpectedly high harmonics [2, 3], and its shape was observed to have a plateau extending non-perturbatively over many orders of magnitude – a process known as *high harmonic generation* (HHG) [4, 5]. The light emitted in this manner is coherent and may reach the extreme ultraviolet and soft X-ray frequency regime opening the path towards the coherent manipulation and control of matter at its natural time scale. These properties can be of paramount importance for many technological and scientific purposes in ultrafast sci-

ence – most notably, the generation of attosecond pulse trains or single isolated attosecond pulses, or the external seeding of free-electron lasers [6, 7, 8]. These advances allow to follow the electron dynamics [9]. Unsurprisingly, a big effort has been devoted to first understanding the underlying physics, and then to controlling and fine-tuning the efficiency and spectral characteristics of the harmonic radiation. The latter can be done by modifying the non-linear medium, or by post-processing the signal with filters, gratings, etc. However, one advantageous alternative is to modify the characteristics of the parent pulse, which obviously will modify the spectral outcome. The most obvious manner of doing this is by systematically varying the defining parameters of this parent pulse [10, 11, 12]. However, the current availability of advanced pulse shaping tools [13], together with the development of closed-loop quantum control techniques [14], provides a superior optimization alternative [15]. In this manner, the successful selective enhancement of harmonic orders could be achieved when using a hollow fiber container for the generating medium [16, 17, 18]. Gas jet (*free focusing*) geometries were also employed [19, 20, 21], but although some degree of control could be achieved (for example, the extension of the cut-off frequency), the very selective order enhancement or depletion obtained with the hollow fibers was not observed. This fact seems to imply that this type of selective enhancement cannot be explained from the single-atom response only; instead, the propagation effects present in the capillary set-up apparently play a fundamental role. In this context. quasiphase matching (QPM) approach is commonly used to achieve independent phase control between multiple high-harmonics [22].

However, a full interpretation of the optimisation mechanisms can only be achieved with theoretical input, for which purpose one may utilise quantum simulations in combination with the theoretical branch of quantum optimal control [23, 14] (QOCT). Recently, Schaefer and Kosloff [24, 25] have addressed this task, showing the possibility of enhancing the emission at desired frequencies for simple few level systems and one-dimensional one.electron system. Here we address, by first principles simulations based on time-dependent density functional theory, the role of many electron interactions in the high harmonic generation, and provide compelling evidence that a single-atom HHG emission can be enhanced by few orders of magnitude in a controlled manner, with standard laser shaping techniques available in many experimental labs.

The *three-step* model successfully describes the key features of HHG [26, 27, 28], at least qualitatively. It combines a quantum description of the ionisation and recombination of the electrons, with a classical description of the intermediate electronic propagation. Lewenstein *et al* [29] developed an approximate, mostly analytical, quantum description based on the *strong field approximation* (SFA): it neglects the contribution of excited bound states, the depletion of the ground state, and considers the continuum electrons to be free of the influence of the parent ion. A more precise approach consists of propagating Schrödinger's equation [30, 31, 32], an expensive method that quickly becomes prohibitive as we increase the number of electrons. For one-electron problems the approach is perfectly feasible, and this fact has encouraged the use of the *single active electron* approximation (SAE), which assumes that only one electron is significantly disturbed by the field, and its evolution may be computed on the combination of the laser field and the potential originating by the parent ion.

This single electron picture is commonly used to describe recollision processes and HHG in atoms and relies on the fact that under HHG conditions there is one electron being ionised. However this doesn't imply the other electrons do not play a role. There is indeed no formal justification for the use of the SAE and in fact, many-body effects have been shown recently to play an important role in HHG providing an explanation of why heavier atoms emit stronger HHG than lighter ones [33] and the giant enhancement of He HHG at 100 ev [34]. However, the SAE has been successful in explaining a few features of the HHG spectra such as the spectral

cutoff, the phase structure of the spectrum and the prediction of the generation of attosecond pulses.

In spite of all those experimental and theoretical efforts, it is clear that the topic of selective HHG generation deserves further microscopical analysis, and in this work, we explore the optimisation possibilities of one and two electron systems (the Hydrogen and the Helium atoms), isolating the single atom response, so that we can learn how much selectivity in the HHG spectrum can be obtained from isolated atoms that can nicely complement QPM schemes in enhancing further the HHG selective emission. For this purpose, we employ a global optimisation scheme that acts on the envelope of the generating pulse, maintaining the fundamental frequency and minimising undesired ionisation (and for molecules also dissociation) processes. For the case of Helium, we report results obtained both with the single active electron approximation, and with time-dependent density-functional theory (TDDFT) [35, 36], in order to assess the influence of the electron-electron interaction in the optimisation process. As many-electron effects may be relevant, TDDFT appears as the ideal framework to capture them in the HHG spectra (see for example Ref. [37]) as it combines a very good compromise between accuracy and computational efficiency. The present optimisation scheme has been implemented in the first-principles code `octopus` [38, 39], that allows the treatment of more complex molecular and extended systems. However for the purposes of the present work, it is better to stay at the simplest level of one and two electron systems. Larger electronic systems would offer a wider range of possibilities for HHG enhancement.

2. Theory

Within the dipole approximation and in the length gauge, the experimentally measured harmonic spectrum can be theoretically approximated by the following formula:

$$H(\omega) = |\int_0^T dt\, \frac{d^2}{dt^2}\langle\hat{\vec{\mu}}\rangle(t)e^{-i\omega t}|^2, \tag{1}$$

i.e. the power spectrum of the second derivative of the expectaction value of the dipole moment $\hat{\vec{\mu}} = -\sum_{i=1}^{N}\hat{\vec{r}}_i$ (although see Ref. [40] for a discussion on the pertinence of using, alternatively, the first derivative or the dipole moment itself). This object is given by:

$$\frac{d^2}{dt^2}\langle\hat{\vec{\mu}}\rangle(t) = \langle\sum_{i=1}^{N}\nabla v(\hat{\vec{r}}_i)\rangle + N\varepsilon(t)\vec{\pi}, \tag{2}$$

where v is the (static) ionic potential, N is the number of electrons, $\varepsilon(t)$ is the laser pulse electric field, and $\vec{\pi}$ is the polarization vector (see the Methods appendix below for some extra details about the theory). Note that this expression can be read as both the acceleration of the electronic system, and as the corresponding back-reaction of the nucleus (or nuclear center of mass, if we are dealing with a molecule). This is not surprising since the electromagnetic emission must be related with a charge acceleration. The expression corresponds, except for the mass factor, with the classical *force* acting on the nucleus, considered as a point particle. We will therefore rewrite Eq. (1) as:

$$H(\omega) = |\vec{f}(\omega)|^2. \tag{3}$$

where $\vec{f}(\omega) = \int_0^T \vec{f}(t)e^{-i\omega t})$ is the Fourier transform of:

$$\vec{f}(t) = \langle\sum_{i=1}^{N}\nabla v(\hat{\vec{r}}_i)\rangle + N\varepsilon(t)\vec{\pi}. \tag{4}$$

From a TDDFT perspective, the use of this force functional is convenient since it can be explicitly written as a density functional:

$$\vec{f}(t) = \int \mathrm{d}^3 r \, n(\vec{r},t) \nabla v(\vec{r}) + N \varepsilon(t) \vec{\pi}. \tag{5}$$

Usually, the electric field $\varepsilon(t)$ is factorised into a sinusoidal function determining the fundamental frequency ω_0, and an *envelope* function f that determines the overall laser-pulse shape:

$$\varepsilon(t) = f(t) \sin(\omega_0 t). \tag{6}$$

This factorisation – and the concept of a *fundamental frequency* – is meaningful for long and quasi-monochromatic pulses, but as the technology has reached the optical period limit, it has started to lose its relevance. Nevertheless, the existence of a fundamental frequency is implicit when speaking of harmonics, which are defined as radiation at integer multiples of precisely that frequency. These will only be well defined if the envelope function is *smooth* compared to the sinusoidal term, i.e. its frequencies are much lower than ω_0.

Therefore, in this work, we investigate the possibility of manipulating the envelope function f, leaving the sinusoidal factor $\sin(\omega_0 t)$ unchanged, in order to influence the shape of the HHG spectrum. This manipulation cannot be unconstrained, as the envelope must be composed of frequencies much lower than ω_0. Moreover, we have searched for solutions that preserve the fluence or total integrated energy of the pulse:

$$\bar{I} = \int \mathrm{d}t \, \varepsilon^2(t). \tag{7}$$

This type of requirement of a specific structure for the solution field (in terms of frequencies, fluence, etc.) can be respected following essentially two routes: by imposing penalties on undesired features of the pulses in the definition of the optimising function, or by constraining from the beginning the search space. This latter option can be achieved by establishing a parametrisation of the control field (in this case, the envelope) that enforces the required condition, and is the route that we have chosen for this work. The search for the optimum is in this manner performed in the space of parameters that determine the control field; the remaining necessary ingredient is the definition of a *merit* function that encodes the physical requirements. Moreover, the assumption of low frequencies for f implies that the spectrum of ε is concentrated around ω_0. Therefore, the $N\varepsilon(t)\vec{\pi}$ term in Eqs. (2), (4), and (5) does not contribute to the HHG spectrum in the region we are interested in and in the following we will safely ignore it.

We have shown how the HHG spectrum may be explicitly computed solely in terms of the system electronic density $n(\vec{r},t)$. For systems with more than one electron, this fact is convenient since it allows to use time-dependent density-functional theory [35, 36] (TDDFT) (see Methods). One can substitute the propagation of the real interacting system by the propagation of a system of fictitious non-interacting electrons whose density is however identical to that of the real one, despite the fact that its wave function is a single Slater determinant.

Hereafter, we will restrict the discussion to one and two-electron systems, the extension to systems with larger number of electrons is straightforward in the TDDFT framework. The one-electron case obviously does not need a TDDFT treatment, although it may be treated as such by considering one single occupied orbital. For such one-orbital problem, the exchange and correlation potential must cancel the Hartree term:

$$v_{\mathrm{xc}}[n](\vec{r},t) = -v_{\mathrm{H}}[n](\vec{r},t), \tag{8}$$

so that the resulting equation reduces to the initial Schrödinger equation. For two-electron systems, we use the exact-exchange approximation (EXX) to the xc term, which for this two-

electron case amounts to setting:

$$v_{\text{xc}}[n](\vec{r},t) = -\frac{1}{2} v_{\text{H}}[n](\vec{r},t), \qquad (9)$$

Note that in this form TDDFT is identical to time-dependent Hartree-Fock that provides a food description of the non-linear properties of two-electron systems except for the description of charge-transfer excitations (see for example Ref. [41]).

The electric field amplitude will be determined by the specification of a set of M parameters $u_1, \ldots, u_M \equiv u : \varepsilon(t) = \varepsilon[u](t)$. The evolution of the TDKS system is in consequence also governed by the choice of parameters u, i.e. the orbitals and density are functionals of the parameters: $u \to \varphi[u]$, $u \to n[u]$. We may then use the tools of QOCT to find the set u that maximizes a given target function G, defined in terms of a functional of the density of the system, i.e.:

$$G[u] = \tilde{F}[n[u]]. \qquad (10)$$

This functional $\tilde{F}$ is designed to favour the desired behaviour of the system (in this case, a certain form of the HHG spectrum, to be detailed below). Note that it is defined in terms of the system density, and not in terms of the full many-body wave function. This definition ensures that the substitution of the real by the Kohn-Sham system in the optimization entails no further approximation. The theory must however be developed in terms of a functional of the Kohn-Sham orbitals, which can be easily defined as:

$$F[\varphi] = \tilde{F}[\mu \varphi^* \varphi], \qquad (11)$$

where μ is the occupation of the orbital, i.e. one or two for one- or two-electron calculations, respectively.

We must now choose a form for F in such a way that its maximization leads to the desired HHG optimization, namely the selective increase of one harmonic peak – that should leave the neighboring ones as low as possible. There is substantial liberty to design F, and it is not evident what functional form should lead to better results.

$$F[\varphi] = \sum_k \alpha_k H[\varphi](k\omega_0), \qquad (12)$$

where α_k takes a positive value for the harmonic to be enhanced, and negative values for the ones that we wish to reduce. However, this choice proved to be problematic, since the modulation of the source signal with the envelope function leads to displacements, sometimes substantial, of the harmonic peaks with respect to the precise integer multiples $k\omega_0$. A general definition that solves this problem (and that includes the previous one as a particular case), is:

$$F[\varphi] = \int d\omega \alpha(\omega) H[\varphi](\omega) = \int d\omega \alpha(\omega) |\vec{f}[\varphi](\omega)|^2, \qquad (13)$$

where we have made explicit the fact that both H and $\vec{f}$, defined in Eqs. (1) and (4) are functionals of the time-dependent evolution for the system. The function α permits to establish some finite window around each harmonic peak $k\omega_0$, that will be positive for the harmonic orders that we want to enhance, and negative for the ones that we want to reduce. Finally, a third option is to seek for the maximum of the spectrum in these frequency windows around the harmonic orders, i.e.:

$$F[\varphi] = \sum_k \alpha_k \max_{\omega \in [k\omega_0 - \beta, k\omega_0 + \beta]} \{\log_{10} H[\varphi](\omega)\}, \qquad (14)$$

where the real number β determines the size of the window.

Once the function G has been defined (through the definition of the target functional F), it remains to use some optimization algorithm to find the optimal u set. There are numerous options, and we may divide them on two groups, depending on whether or not they require the computation of the gradient of G – in addition of the computation of the function itself. The methods that employ the gradient are of course more efficient, as long as this gradient can itself be computed efficiently. The simplest scheme is steepest descents, but one can also use conjugate gradients or, in our case, the Broyden-Fletcher-Goldfarb-Shanno (GFBS) quasi-Newton method.

For the function G, the gradient is given by [42]:

$$\nabla G[u] = 2 \int_0^T \mathrm{d}t \ \nabla \varepsilon[u](t) \mathrm{Im}\langle \chi[u](t) | \hat{\vec{r}} \cdot \hat{\pi} | \varphi[u](t) \rangle. \tag{15}$$

This expression uses an auxiliary orbital $\chi[u]$ defined by the following equations of motion:

$$
\begin{aligned}
\mathrm{i}\frac{\partial}{\partial t}\chi[u](\vec{r},t) &= -\frac{1}{2}\nabla^2\chi[u](\vec{r},t) + v_{\mathrm{KS}}^*[n[u]](\vec{r},t)\chi[u](\vec{r},t) \\
&\quad + \hat{K}[\varphi[u](t)]\chi[u](\vec{r},t) \\
&\quad - i\frac{\delta F[\varphi[u]]}{\delta\varphi^*[u](\vec{r},t)}, \tag{16}
\end{aligned}
$$

$$\chi[u](\vec{r},T) = 0. \tag{17}$$

The operator $\hat{K}[\varphi[u][t]]$ is defined as:

$$\hat{K}[\varphi[u](t)]\chi[u](\vec{r},t) = -4\mathrm{i}\varphi[u](\vec{r},t)\mathrm{Im}\int \mathrm{d}^3 r' \ \chi^*[u](\vec{r}',t)f_{\mathrm{Hxc}}[n[u](t)](\vec{r},\vec{r}')\varphi[u](\vec{r}',t), \tag{18}$$

where f_{Hxc} is the so-called *kernel* of the Kohn-Sham Hamiltonian, which, for our two-electron case treated within the EXX approximation, is given by: $f_{\mathrm{Hxc}}[n](\vec{r},\vec{r}') = \frac{1}{2}\frac{1}{|\vec{r}-\vec{r}'|}$, and is null for the one-electron case (zeroing the full $\hat{K}$ operator).

The functional derivative of F, needed in Eq. (16), for the HHG target defined in Eq. (13), is:

$$\frac{\delta F}{\delta\varphi^*(\vec{r},t)} = \vec{g}[\varphi](t) \cdot \nabla v(\vec{r}) \ \varphi(\vec{r},t), \tag{19}$$

where $\vec{g}[\varphi](t) = 2\mu \int \mathrm{d}\omega \ \alpha(\omega)\mathrm{Re}\left[\vec{f}[\varphi](\omega)e^{-i\omega t}\right]$.

However, we cannot compute this functional derivative for the target defined in Eq. (14) due to the presence of the "max" function, at least in a simple and efficient manner. In consequence, when using this target definition we could not make use of any of the optimization algorithms that make use of the gradient, and turned to the gradient-free NEWUOA algorithm [43], which is a very efficient scheme for optimization problems with a moderate number of degrees of freedom, such as the ones treated here.

In fact, for the optimizations attempted in this work, we observed numerically that the target of Eq. (14) provided much better results than the target of Eq. (13), and therefore we will only show below gradient-free optimizations; in a forthcoming publication, where the target is the HHG cut-off extension, we will present gradient-based optimizations based on a target of the type given in Eq. (13).

Therefore, it remains to specify the set of parameters u that determine the envelope of the electric fields. The requirements are: (i) the envelope should have a given cut-off frequency; (ii) the field should smoothly approach zero at the end points of the propagation time interval; (iii) the total integral of the field should be zero, and (iv) the *fluence* or total integrated intensity of

the pulse should have a constant pre-defined value. This last condition is merely a choice, and not a physical constraint that experimentalists face.

The first step to parametrize the applied time-dependent electroc field $\varepsilon(t)$ in order to enforce all these constraints is to expand the envelope in a Fourier series:

$$f(t) = \sum_{i=1}^{2L} f_i g_i(t),\tag{20}$$

where

$$g_i(t) = \begin{cases} \sqrt{\frac{2}{T}}\cos\left(\frac{2\pi}{T}it\right) & (i=1,\dots,L) \\ \sqrt{\frac{2}{T}}\sin\left(\frac{2\pi}{T}(i-L)t\right) & (i=L+1,\dots,2L) \end{cases}\tag{21}$$

This series fixes the maximum possible (*cut-off*) frequency to $\frac{2\pi}{T}L$. Note that it explicitly omits the zero-frequency term, which is a desired restriction, in order to fulfill: $\int_0^T \mathrm{d}t\, f(t) = 0$.

The manifold spanned by the f_i coefficients is not yet, however, our parameter space, since we still want to enforce the conditions $f(0) = f(T) = 0$, and fix the fluence: $\bar{I} = \int \mathrm{d}t\, \varepsilon^2(t) = \bar{I}_0$. As discussed in Ref. [44], these conditions reduce the degrees of freedom from $2L$ to $2L-2$: the final parameters $u_1,\dots u_{2L-2}$ are finally the hyperspherical angles that characterize a sphere of constant fluence, determining the Fourier coeffiencients: $f_i = f_i[u]$.

In all the OCT calculations to be shown below we have fixed the wavelength of the fundamental frequency ω_0 to 800 nm, a very common value used in laboratories equipped with a Ti:sapphire source. The total pulse duration is fixed to 200 cycles, $T = 200\, 2\pi/\omega_0$, which corresponds to 533 fs approximately. The envelope function $f(t)$ is then restricted to have frequencies no larger than $\omega_0/60$. The fluence [Eq. (7)] is then fixed to a value (around 5.0 a.u.) that ensures a sufficiently non-linear response of both the Hydrogen and Helium atoms, while not causing a substantial ionization. Fixing the fluence does not imply fixing the peak intensity; however the simultaneous existence of a maximum frequency puts a limit on it; in practice, the peak intensities observed in the optimal pulses are in the range of $5\ 10^{13}$ - 10^{14} W/cm^2.

The optimization are started from randomly generated sets of parameters u. Since the procedure finds local maxima, we have performed several searches for each case, choosing afterwards the best among them. In order to have some "reference" to compare the optimal run to, we define a reference pulse as:

$$\varepsilon_{\text{ref}}(t) = \varepsilon_0 \cos\left(\frac{\pi}{2}\frac{2t-T}{T}\right)\cos(\omega t),\tag{22}$$

i.e. a cosinoidal envelope that peaks at $t = T/2$ with a value of ε_0, chosen to fulfill the fluence condition.

3. Results

The calculated HHG spectrum emitted by the Hydrogen and Helium atoms, irradiated by the reference pulse, is depicted in Fig. 1. Note that there is a range of harmonics with comparable intensities forming a plateau (9 to 19 in H and 15 to 21 in He). Because of this, we have selected that range (shaded in the plot) to perform the selective optimisations. The range is displayed, this time with a linear y axis scale, in the inset. For the case of He we show the EXX and SAE results. As in He two electrons populate the only orbital in a spin-compensated configuration, the SAE approximation, in this case, consists in neglecting the interaction between the electrons during the action of the field, freezing the potential to its ground state shape. In this adiabatic-DFT context, it amounts to ignoring the time-evolution of the Hartree, exchange and
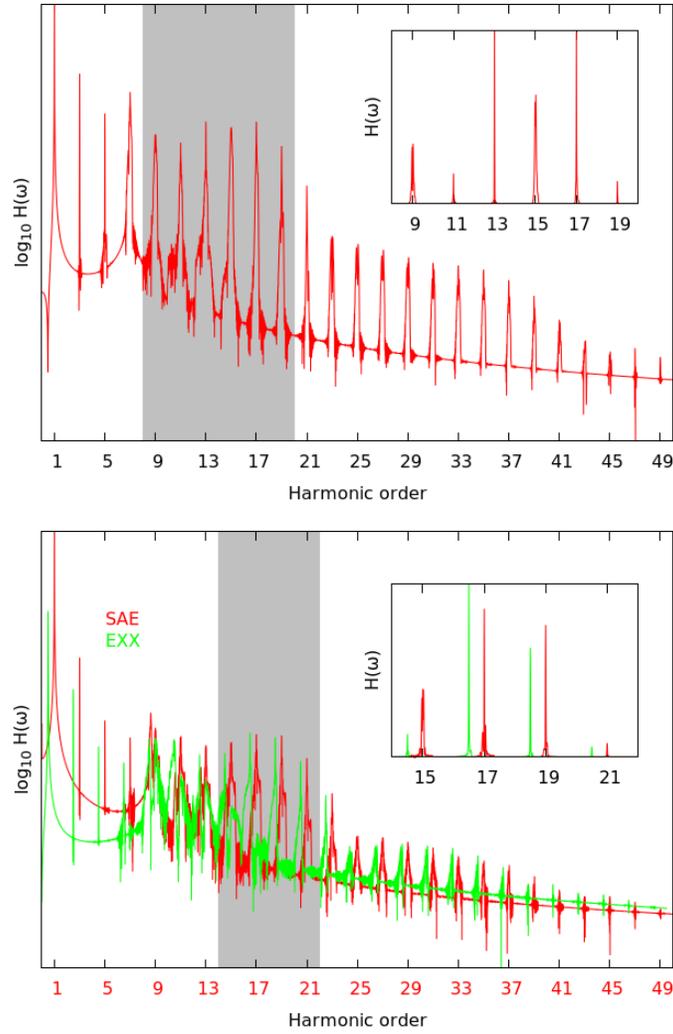
Fig. 1. HHG spectrum of the Hydrogen (top) and He (bottom) atoms, with the reference pulse of Eqn. (22. For the case of the He HHG spectra we show two results: one solving the TDDFT equations using the EXX functional (green) and the other solving the single-active-electron (SAE) (red) equation, commonly used by the strong-field community. To make more clear the comparison between EXX and SAE we shifted the SAE spectra by $0.5\omega_0$ in the x-axis. The shaded area contains the harmonics of interest. This area is also displayed in the inset, with a linear y-axis scale.

correlation potentials, and is useful to gauge the relevance that correlations may have on the HHG optimisation.

Let's discuss first the case of optimising the HHG spectra of H. We used the target given by Eq. (14) to optimise the odd orders from the 9th to 19th. To enhance the 9th harmonic, for example, we set $\alpha_9 = 5$, and $\alpha_{11} = \alpha_{13} = \alpha_{15} = \alpha_{17} = \alpha_{19} = -1$ (all other α_k are zero). In this manner, the sum of all coefficients is zero, avoiding any improvement of the merit function due to a mere overall reduction or increase of the spectrum. The results are displayed in Fig. 2. From top to botton, in the left panels, the spectra produced by the optimal fields for the 19th, 17th, ..., 9th harmonic. In the right panels, the optimal fields themselves; their envelopes in real time, as well as their power spectrum.

The resulting fields produce considerably higher harmonic outputs than the unshaped, reference field. To quantify this point we introduced an *enhancement factor* that is displayed in each plot, defined as:

$$\kappa_j = \frac{\max_{\omega \in [k\omega_0 - \beta, k\omega_0 + \beta]} \{H[\varphi](\omega)\}}{H_{\text{ref}}(j\omega_0)}, \tag{23}$$

where H_{ref} is the spectrum obtained with the reference field, and H the one obtained with the optimal field (the computation of the max function is not needed for the former, because due to the regularity of its envelope function, H_{ref} always peaks at the precise integer multiples $j\omega_0$). This enhancement factor greatly vary from case to case (i.e. it is 6 for $j = 13$, and 208 for $j = 15$). Note that the plots do not share the same y-scale; they are scaled in each case to the value of the maximum of the plot.

We turn now our attention to the case of the Helium atom, that contains two electrons. The interaction between these is treated here with TDDFT, within the EXX approximation. As in the previous case we performed optimisations based on the target given by Eq. (14), now for the orders 15th to 21st, fixing the coefficients α_k in an analogous manner. The results are displayed in Fig. 3. From top to bottom, in the left panels, the spectra produced by the optimal fields for the 21st, 19th, 17th, and 15th harmonic. In the right panels, the optimal fields themselves.

The enhancement factors achieved are quite large, and as in the case of Hydrogen, rather different from case to case. This rather large enhancement of the wanted harmonic is not accompanied by a full depletion of the neighbouring ones – in fact, they are also increased. This partial selectivity is also similar to the Hydrogen results. To quantify the role of electron-electron interactions we show in the same Fig. 3 the SAE results (red curve). Qualitatively, the SAE results are not very different to the ones obtained with the EXX functional, in terms of intensity enhancements and selectivity. The fact that the calculated optimal fields and the spectra are different for both EXX and SAE illustrate not only the intrinsic non-linearity of the optimisation algorithms and the rather large number of possible local maxima, but also the fact that electron interaction does play a role in the generation and optimisation of harmonics. Indeed, by looking in more detail to the results shown in Fig. 3 for the 15th and 19th harmonic optimisation, we see that EXX with respect to SAE provides a better selectivity and harmonic enhancement, measured by the height of the desired harmonic and the quenched of the neighbouring ones. Therefore electron correlation seems to play a role in the optimisation of harmonics. This fact, together with the common knowledge that heavier noble gases emit stronger HHG radiation that light ones (whereas the SAE that predicts similar spectra) [45, 46, 47] support our findings about the limitations of the SAE approximation and the role of electron interactions. In fact we can expect larger enhancement factors to be reached by applying the present optimisation techniques to heavier atomic/molecular systems.
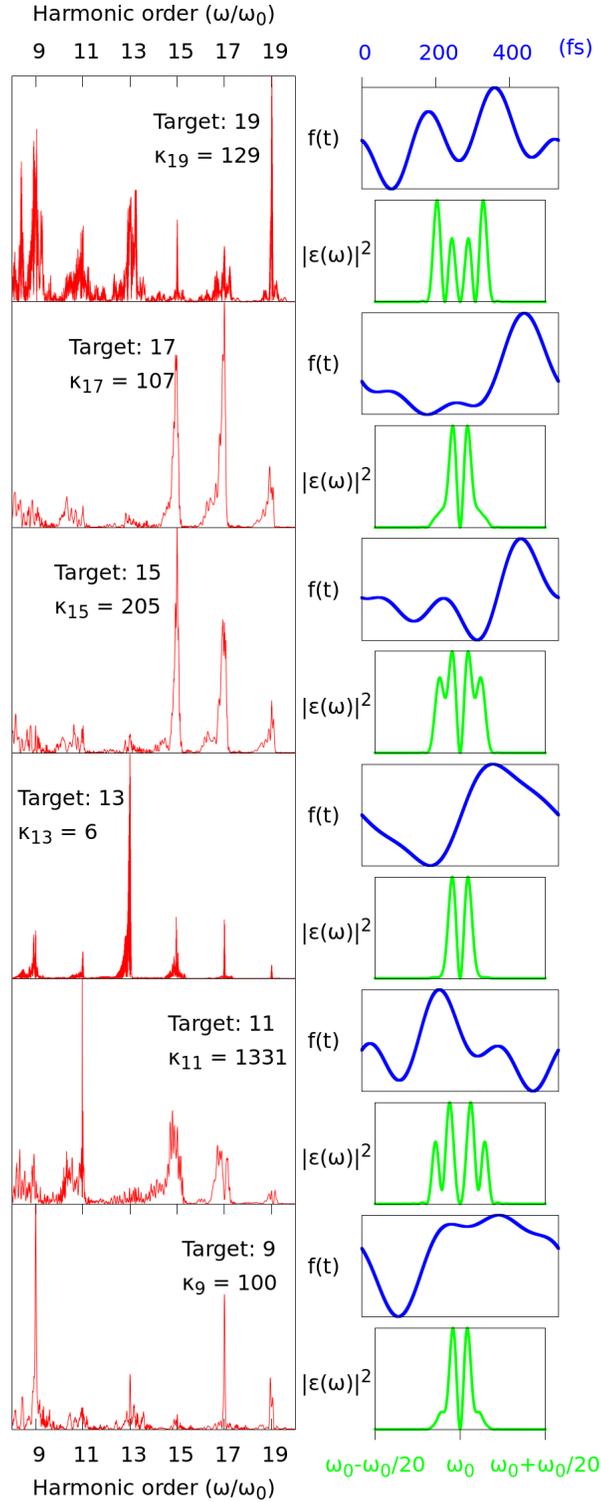
Fig. 2. Optimized HHG spectra (left panels), and corresponding optimal fields (right panels), for the Hydrogen atom case. The optimal fields are plotted in the time domain (only the envelope function $f(t)$ is shown), and in the frequency domain. The HHG spectra are shown in a linear scale, normalized in each case up the value of the maximun value. The enhancement factor defined in Eq. (23) is also shown.
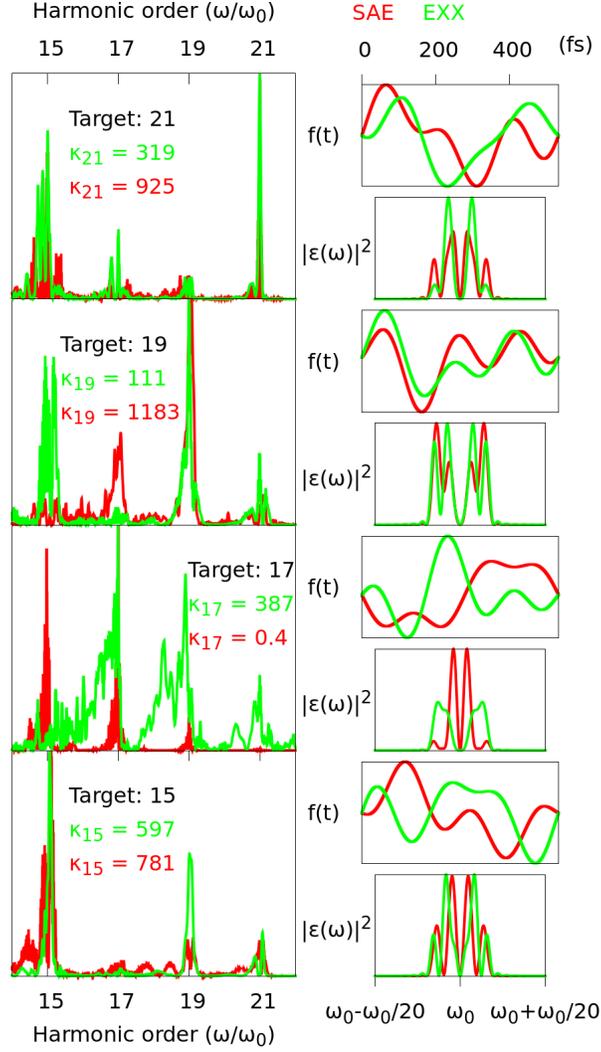
Fig. 3. Optimized HHG spectra (left panels), and corresponding optimal fields (right panels), for the Helium atom case. As in Fig. (1) we show in green the results within TDDFT using the EXX functional and in red the ones using the SAE approximation. The optimal fields are plotted in the time domain (only the envelope function $f(t)$ is shown), and in the frequency domain. The HHG spectra are shown in a linear scale, normalized in each case up the value of the maximun value. The enhancement factor defined in Eq. (23) is also shown.

4. Conclusion

In conclusion, we have investigated, by theoretical means, the possibility of tuning the shape of the HHG spectrum of the Hydrogen and Helium atoms by shaping the slowly varying envelope of a 800 nm, 200-cycles long laser pulses. For this purpose, we have optimised a functional designed to enhance selected harmonics. The allowed modifications of the pulse are very constrained, since we enforce a maximum envelope frequency no larger than 1/60 of the fundamental frequency. This means very slowly varying envelopes. However, the picture that emerges of our analysis is that these relatively small modifications produce strong variations of the spectra, allowing for significative increases of the harmonic intensities. These enhancements are not fully selective, since the neighbouring harmonics also increase, but to a lesser extent. The outcome depends of the precise definition of the target functional, which is a topic to be investigated further. There is ample freedom to choose this object, and a different option may yield better selectivity – while perhaps reducing the total enhancement, or vice-versa.

The spectra have been computed with a fully quantum mechanical description, by explicitly computing the time-dependent dipole moment of the systems. The results presented here correspond to the single-atom response – we have not propagated Maxwell's equations in a atomic gaseous medium. Therefore, this work demonstrates the relevance of the single atom response for HHG and how this single-atom response is significantly altered by the envelope of the laser pulse, even for the small modifications allowed in our scheme. We have shown that few orders of magnitude HHG enhancement factor can be reached at the single-atom level. Thus, if this fact is combined with the phase matching method used for HHG generation we would be able to reach much higher global harmonic enhancement in atomic and molecular gases. Moreover, our results illustrate the role of electron-electron interactions in this optimisation and control of HHG. This can be qualitatively rationalised in terms of the larger Hilbert space spanned by the interacting system as compare to the simplest single-active electron scheme (or any other non-interacting electron approach).

Appendix: Methods

The propagation of the TDDFT equations are those of the single-particle orbitals forming the Slater determinant, a set of equations usually called "time-dependent Kohn-Sham" (TDKS) equations:

$$i\frac{\partial}{\partial t}\varphi_i(\vec{r},t) = -\frac{1}{2}\nabla^2\varphi_i(\vec{r},t) + v_{\text{KS}}[n](\vec{r},t)\varphi_i(\vec{r},t),\qquad(24)$$

$$\varphi_i(\vec{r},0) = \varphi_i^{\text{gs}}(\vec{r}).\qquad(25)$$

The initial values specifed by Eqs. (25) are given by the ground-state Kohn-Sham orbitals, computed with static DFT. The time-dependent density of the system may be retrieved from the KS orbitals with the simple formula:

$$n(\vec{r},t) = \sum_{i=1}^{N/2}\mu_i|\varphi_i(\vec{r},t)|^2.\qquad(26)$$

where μ_i is the occupation of each orbital, which is equal to two if we consider a spin-compensated system of N electrons, doubly occupying a set of $N/2$ spatial orbitals φ_i ($i = 1,\ldots,N/2$).

The potential that appears in those equations, v_{KS} (the "Kohn-Sham potential") is a functional of this density, and is defined as:

$$v_{\text{KS}}[n](\vec{r},t) = v(\vec{r}) + \varepsilon(t)\vec{\pi}\cdot\vec{r} + v_{\text{H}}[n](\vec{r},t) + v_{\text{xc}}[n](\vec{r},t),\qquad(27)$$

where the Hartree potential v_H is given by:

$$v_H[n](\vec{r},t) = \int d^3 r' \, \frac{n(\vec{r}',t)}{|\vec{r}' - \vec{r}|},$$ (28)

and $v(\vec{r})$ is the static external potential. The time-dependent external potential for these one-electron equations is given by $\varepsilon(t)\vec{\pi}\cdot\vec{r}$, in terms of objects already defined.

We have studied the two simplest atoms, Hydrogen and Helium. For the Helium atom, we have used TDDFT with the exact-exchange functional. In order to assess the possible relevance of the electron-electron interaction, we have repeated the Helium atom calculations employing the single active electron (SAE) approximation, which in this case amounts to freezing the Hartree, exchange and correlation functional to its ground-state value during the propagations. In this manner, we are effectively ignoring the electron-electron interaction during the propagation, and may gauge the relevance that it may have on the possibility of changing HHG spectra via smooth variations of the envelope function.

For the purpose of studying the HHG of atoms in linearly polarized pulses, one-dimensional (1D) models have been routinely employed in the past, and we have adhered to this practice, since it provides a good qualitative picture, while substantially reduces the computational cost. The nucleus-electron interaction has the soft-Coulomb form:

$$v(x) = -\frac{Z}{\sqrt{a^2 + (x-x_0)^2}}.$$ (29)

for an electron placed at x and a nucleus of charge Z placed at x_0. The constant a may be tuned to reproduce some atomic property (e.g. ionization potential), although in this case we have simply fixed it to one for both Hydrogen and Helium.

Everything has been implemented in the `octopus` code [38, 39]. The wavefunctions, potential, densities, etc. are represented in this code by the values they take at points of a real space grid. The Laplacian operator, needed to compute the kinetic part of the Hamiltonian, is computed using a 9-point finite difference formula. The propagations are performed by dividing the full time interval into short time steps $[t_0, t_1 = t_0 + \Delta t, t_2 = t_0 + 2\Delta t, \ldots, T]$, and approximating the short-time evolution operator $\hat{U}(t_{i+1}, t_i)$ with the exponential mid-point rule:

$$\hat{U}(t_{i+1}, t_i) \approx \exp\{-i\Delta t \hat{H}(t_i + \frac{1}{2}\Delta t)\}.$$ (30)

The action of the exponential on a state vector is computed by making use of the Lanczos polynomial expansion (see Ref. [48] for a discussion of the propagation schemes used in `octopus`). The full details about the combination of TDDFT and QOCT were explained in Refs. [42] and [49].

Acknowledgments